

# Normal state above the upper critical field in $\text{Fe}_{1+y}\text{Te}_{1-x}(\text{Se},\text{S})_x$

Aifeng Wang (王爱峰),<sup>1</sup> Erik Kampert,<sup>2</sup> H. Saadaoui,<sup>3</sup> H. Luetkens,<sup>3</sup> Rongwei Hu (胡荣伟),<sup>1,\*</sup> E. Morenzoni,<sup>3</sup> J. Wosnitza,<sup>2,4</sup> and C. Petrovic<sup>1</sup>

<sup>1</sup>Condensed Matter Physics and Materials Science Department, Brookhaven National Laboratory, Upton, New York 11973, USA

<sup>2</sup>Hochfeld-Magnetlabor Dresden (HLD-EMFL), Helmholtz-Zentrum Dresden-Rossendorf, D-01314 Dresden, Germany

<sup>3</sup>Laboratory for Muon Spin Spectroscopy, Paul Scherrer Institute, CH-5232 Villigen PSI, Switzerland

<sup>4</sup>Institut für Festkörperphysik, Technische Universität Dresden, D-01062 Dresden, Germany

(Received 12 October 2016; revised manuscript received 25 January 2017; published 3 May 2017)

We have investigated the magnetotransport above the upper critical field ( $H_{c2}$ ) in  $\text{Fe}_{1.14}\text{Te}_{0.7}\text{Se}_{0.3}$ ,  $\text{Fe}_{1.02}\text{Te}_{0.61}\text{Se}_{0.39}$ ,  $\text{Fe}_{1.05}\text{Te}_{0.89}\text{Se}_{0.11}$ , and  $\text{Fe}_{1.06}\text{Te}_{0.86}\text{S}_{0.14}$ . The  $\mu\text{SR}$  measurements confirm electronic phase separation in  $\text{Fe}_{1.06}\text{Te}_{0.86}\text{S}_{0.14}$ , similar to  $\text{Fe}_{1+y}\text{Te}_{1-x}\text{Se}_x$ . Superconductivity is suppressed in high magnetic fields above 60 T, allowing us to gain insight into the normal-state properties below the zero-field superconducting transition temperature ( $T_c$ ). We show that the resistivity of  $\text{Fe}_{1.14}\text{Te}_{0.7}\text{Se}_{0.3}$  and  $\text{Fe}_{1.02}\text{Te}_{0.61}\text{Se}_{0.39}$  above  $H_{c2}$  is metallic as  $T \rightarrow 0$ , just like the normal-state resistivity above  $T_c$ . On the other hand, the normal-state resistivity in  $\text{Fe}_{1.05}\text{Te}_{0.89}\text{Se}_{0.11}$  and  $\text{Fe}_{1.06}\text{Te}_{0.86}\text{S}_{0.14}$  is nonmetallic down to lowest temperatures, reflecting the superconductor-insulator transition due to electronic phase separation.

DOI: 10.1103/PhysRevB.95.184504

## I. INTRODUCTION

It is important to understand the normal state of iron based superconductors since the mechanism of conductivity carries the information about the interactions and correlations in the electronic system out of which superconductivity develops [1–4]. The conductivity, however, is often connected with crystal lattice imperfections or defects. Granular Al-Ge films host superconducting Al islands embedded in an amorphous Ge matrix [5,6]. In underdoped copper oxides such chemical (crystallographic) phase separation on two space groups is absent, yet the inhomogeneous hole concentration induces nanoscale phase separation into superconducting domains and electronically distinct background [7]. Both granular aluminum and underdoped copper oxides feature a metallic state above zero-field  $T_c$ . Magnetic-field induced breakdown of superconductivity is expected to give rise to a metallic state below the zero-field  $T_c$  in a conventional superconductor. However, upon applying pulsed magnetic fields, a superconductor-insulator transition (SIT) was reported in both granular aluminum and underdoped copper oxides such as  $\text{La}_{2-x}\text{Sr}_x\text{CuO}_4$ ,  $\text{Bi}_{2}\text{Sr}_{2-x}\text{La}_x\text{CuO}_6$ , and  $\text{Pr}_{2-x}\text{Ce}_x\text{CuO}_{6+\delta}$  [6,8–10]. The mechanism of the SIT can stem not only from the Coulomb interaction enhanced by disorder within the BCS framework but also from granularity [11–13]. In granular superconductors, which feature isolated superconducting grains, Josephson tunneling between the grains establishes the macroscopic superconducting state.

The Fe-based superconductors share many similarities with copper-oxide superconductors, such as the layered crystal structure and superconductivity that emerges by the suppression of an antiferromagnetic ground state [14,15]. Although still quite scarce due to the high upper critical fields, studies of the normal-state electronic transport in FeAs-based superconductors below zero-field  $T_c$  have revealed  $\log T$

nonmetallic resistivity that is unrelated to SIT [16]. Such studies are also infrequent for FeSe-based superconductors. Yet due to the complexity of nanoscale inhomogeneity iron-selenide materials offer an opportunity to correlate conducting states below zero-field  $T_c$  in high magnetic fields with the aspects of crystal structure.  $\text{K}_x\text{Fe}_{2-y}\text{Se}_2$  superconductors feature a crystal structure that is phase separated in two space groups where electronic phase separation comes naturally in superconducting islands immersed in an insulating matrix, just like in granular aluminum [17–21]. On the other hand and similar to copper oxides,  $\text{Fe}_{1+y}\text{Te}_{1-x}\text{Se}_x$  superconductors exhibit an electronic phase separation below zero-field  $T_c$  whereas their crystal structure is chemically inhomogeneous but not phase separated since they crystallize in one space group with defects and interstitial atoms irrespective of Se/Te ratio [22–31]. Whereas a SIT has been reported in doped  $\text{K}_x\text{Fe}_{2-y}\text{Se}_2$  [32,33], the nature of the conducting states below zero-field  $T_c$  for  $H > H_{c2}$  is still unknown in  $\text{Fe}_{1+y}\text{Te}(\text{Se},\text{S})_x$ .

The normal-state resistivity reflects the electronic structure underlying the high-temperature superconductivity and hints at the origin of its mechanism [34]. It is of interest to understand the normal state of FeCh (Ch = S, Se, or Te) in high magnetic fields since  $\text{FeCh}_4$  tetrahedra constitute potential building blocks of high-temperature superconductivity. Bulk  $\beta$ -FeSe superconducts below 8.5 K [35]. This can be enhanced up to 15 K by Te doping in bulk  $\text{Fe}_{1+y}\text{Te}_{1-x}\text{Se}_x$  or up to about 30 K by pressure or in  $\text{K}_x\text{Fe}_{2-y}\text{Se}_2$  [28,36,37]. FeSe films on  $\text{SrTiO}_3$  have shown  $T_c$  as high as 100 K [38].

The doping-dependent phase diagrams of  $\text{Fe}_{1+y}\text{Te}_{1-x}\text{Se}_x$  and  $\text{Fe}_{1+y}\text{Te}_{1-x}\text{S}_x$  indicate a superconducting dome as a function of Se or S doping on the Te site [22,23]. They also suggest an electronic phase separation below zero-field  $T_c$  in superconducting and magnetic volume fractions. This allows for the investigation of SIT in FeSe superconductors with no crystallographic phase separation inherent to  $\text{K}_x\text{Fe}_{2-y}\text{Se}_2$ .

In this paper we have examined the normal state in high magnetic fields when superconductivity is suppressed for  $x = 0.14$  sulfur and  $x = 0.11, 0.30, 0.39$  of Se substitution. We compare the normal-state transport below zero-field  $T_c$  in

\*Present address: Rutgers Center for Emergent Materials and Department of Physics and Astronomy, Rutgers University, Piscataway, NJ 08854, USA.

high magnetic fields for materials with different normal-state transport above  $T_c$  (metallic versus nonmetallic) and with different amounts of interstitial Fe which favors Kondo-type scattering. These crystals exhibit a different electronic phase separation below zero-field  $T_c$ . The volume fractions of superconductivity are about 1% for  $x = 0.11$  Se and about 10% for  $x = 0.30$  and 0.39 Se [22]. We show electronic phase separation below zero-field  $T_c$  in  $\text{Fe}_{1.06}\text{Te}_{0.86}\text{S}_{0.14}$ , similar to  $\text{Fe}_{1+y}\text{Te}_{1-x}\text{Se}_x$  [22]. We also show that the normal state in  $\text{Fe}_{1.05}\text{Te}_{0.89}\text{Se}_{0.11}$  and  $\text{Fe}_{1.06}\text{Te}_{0.86}\text{S}_{0.14}$  below zero-field  $T_c$  above  $H_{c2}$  is nonmetallic whereas the in-plane resistivity below  $T_c$  for  $\text{Fe}_{1.14}\text{Te}_{0.7}\text{Se}_{0.3}$  and  $\text{Fe}_{1.02}\text{Te}_{0.61}\text{Se}_{0.39}$  is metallic for  $H > H_{c2}$ , just like the normal-state resistivity above the  $T_c$ . In the absence of Kondo-type scattering [39,40], which is suppressed in high magnetic fields, the results for  $\text{Fe}_{1.05}\text{Te}_{0.89}\text{Se}_{0.11}$  and  $\text{Fe}_{1.06}\text{Te}_{0.86}\text{S}_{0.14}$  show clear SIT behavior [12,13]. This is an observation of SIT in electronically granular Fe superconductors in the absence of crystallographic phase separation, similar to copper oxides.

## II. EXPERIMENT

The single crystals used in this paper were grown and characterized as described previously [23,41]. Pulsed-field experiments were performed up to 61 T using a magnet with 150-ms pulse duration at the Dresden High Magnetic Field Laboratory. The magnetic field is applied parallel to the  $c$  axis to most effectively suppress superconductivity. Data were obtained via a fast data-acquisition system operating with ac current in the kHz range. The exposure of the samples to ambient conditions was minimized by handling the samples in a glove box. The contacts were made on freshly cleaved surfaces inside the glove box using silver paint and platinum wires. The elemental and microstructure analyses were performed using energy-dispersive x-ray spectroscopy in a JEOL JSM-6500 scanning electron microscope [23,41]. The average stoichiometry was determined by examination of multiple points on the crystals. The measured compositions were  $\text{Fe}_{1.14(2)}\text{Te}_{0.70(2)}\text{Se}_{0.30(2)}$ ,  $\text{Fe}_{1.02(3)}\text{Te}_{0.61(4)}\text{Se}_{0.39(4)}$ ,  $\text{Fe}_{1.05(3)}\text{Te}_{0.89(2)}\text{Se}_{0.11(2)}$ , and  $\text{Fe}_{1.06(3)}\text{Te}_{0.86(1)}\text{S}_{0.14(2)}$ . The error bars reflect the maximum distance from the average stoichiometry (inhomogeneity). The typical crystal size was about  $4 \times 1 \times 0.2$  mm. The contact resistance was between 10 and 50  $\Omega$  and the excitation current was 0.3 mA, which corresponds to a current density of approximately  $10^3$  A/m<sup>2</sup>, ensuring the absence of resistive heating effects. Transverse-field (TF)- and zero-field (ZF)- $\mu$ SR experiments were carried out at the Paul Scherrer Institute (Villigen, Switzerland) on  $\text{Fe}_{1.05}\text{Te}_{0.89}\text{Se}_{0.11}$  in order to detect and quantify magnetic and superconducting phases. The sample was cooled to the base temperature of 5 K in zero field for the ZF- $\mu$ SR experiments. The ZF- and TF- $\mu$ SR data were analyzed by using the MUSRFIT software package [42].

## III. RESULTS AND DISCUSSION

The normal-state resistivities of  $\text{Fe}_{1.02}\text{Te}_{0.61}\text{Se}_{0.39}$  and  $\text{Fe}_{1.14}\text{Te}_{0.7}\text{Se}_{0.3}$  are metallic, whereas  $\text{Fe}_{1.05}\text{Te}_{0.89}\text{Se}_{0.11}$  and  $\text{Fe}_{1.06}\text{Te}_{0.86}\text{S}_{0.14}$  feature a temperature dependence of an incoherent metal (Fig. 1) [23,39,43]. The resistivity values are

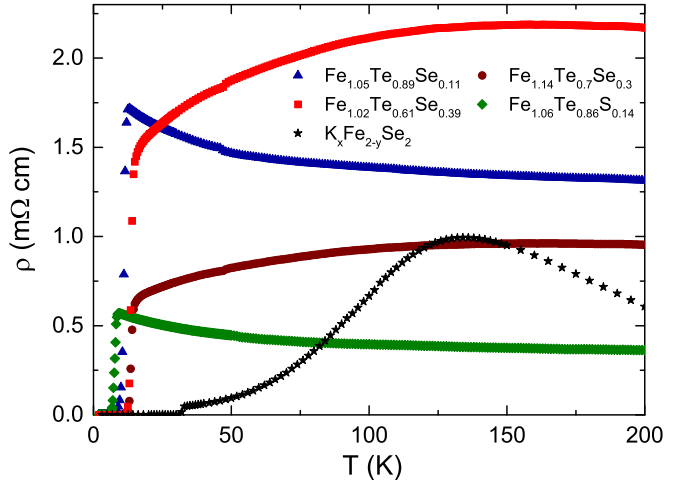


FIG. 1. Temperature dependence of the in-plane resistivity for  $\text{Fe}_{1.02}\text{Te}_{0.61}\text{Se}_{0.39}$ ,  $\text{Fe}_{1.14}\text{Te}_{0.7}\text{Se}_{0.3}$ ,  $\text{Fe}_{1.05}\text{Te}_{0.89}\text{Se}_{0.11}$ , and  $\text{Fe}_{1.06}\text{Te}_{0.86}\text{S}_{0.14}$  single crystals. For comparison we also plot the resistivity of  $\text{K}_x\text{Fe}_{2-y}\text{Se}_2$ .

higher than those of  $\text{K}_x\text{Fe}_{2-y}\text{Se}_2$  where grain boundaries also contribute due to crystallographic phase separation [44]. We note that the mean free path of  $\text{Fe}_{1.14}\text{Te}_{0.91}\text{S}_{0.09}$  is  $l = 1.35$  nm [39]. Assuming similar mean free path for  $\text{Fe}_{1.06}\text{Te}_{0.86}\text{S}_{0.14}$  investigated here and noting that for  $\text{Fe}_{1+y}\text{Te}_{0.5}\text{Se}_{0.5}$  carrier concentration is about  $2 \times 10^{21}$  cm<sup>-3</sup> [45], we see that for resistivities of about 1–2 m $\Omega$  cm, the Drude mean free path  $l = \hbar(3\pi^2)^{1/3}/(e^2\rho_0 n^{2/3})$  should be about 0.3–0.5 nm. This is comparable to the interatomic spacing where the resistivity should saturate [46,47]. Therefore the high-temperature resistivity (Fig. 1) should also be affected by the Mott-Ioffe-Regel saturation similar to  $\text{SrFe}_{2-x}\text{M}_x\text{As}_2$  (M = Co, Ni), in addition to localization and incoherence due to Kondo scattering [23,39,40,43,48].

The magnetoresistances (MRs) at different temperatures for  $\text{Fe}_{1.14}\text{Te}_{0.7}\text{Se}_{0.3}$  and  $\text{Fe}_{1.02}\text{Te}_{0.61}\text{Se}_{0.39}$  are shown in Figs. 2(a) and 2(b). Superconductivity is suppressed by increasing magnetic field at fixed temperature, and the transition in the field-dependent  $\rho_{ab}$  data is shifted to lower magnetic fields with increasing temperature. We observe a finite resistance in the superconducting state of  $\text{Fe}_{1.14}\text{Te}_{0.7}\text{Se}_{0.3}$ , which may be caused either by experimental artifacts or by thermally activated vortex-flux motion. The upper critical fields of  $\text{Fe}_{1.14}\text{Te}_{0.7}\text{Se}_{0.3}$  and  $\text{Fe}_{1.02}\text{Te}_{0.61}\text{Se}_{0.39}$  are about 45 T, consistent with previous reports [41,49]. The temperature dependence of the resistivity of  $\text{Fe}_{1.14}\text{Te}_{0.7}\text{Se}_{0.3}$  and  $\text{Fe}_{1.02}\text{Te}_{0.61}\text{Se}_{0.39}$  is presented in Figs. 2(c) and 2(d). The normal-state resistivity of  $\text{Fe}_{1.14}\text{Te}_{0.7}\text{Se}_{0.3}$  continues to decrease below  $T_c$  and is nearly constant between 4 and 12 K. A similar behavior was observed in  $\text{Fe}_{1.02}\text{Te}_{0.61}\text{Se}_{0.39}$  and  $\text{FeSe}$ , where the high-field resistivity at  $T \leq 1$  K is almost temperature independent [41,50].

Figures 3(a) and 3(b) show how the superconducting transitions of  $\text{Fe}_{1.05}\text{Te}_{0.89}\text{Se}_{0.11}$  and  $\text{Fe}_{1.06}\text{Te}_{0.86}\text{S}_{0.14}$  shift to low field with increasing temperature. Superconductivity is suppressed at all temperatures below zero-field  $T_c$  above 40 T, revealing a nonmetallic normal-state resistivity with decreasing temperature [Figs. 3(c) and 3(d)]. We note that the resistivity as a function of magnetic field near  $H_{c2}$  is nonmonotonic (Fig. 3,

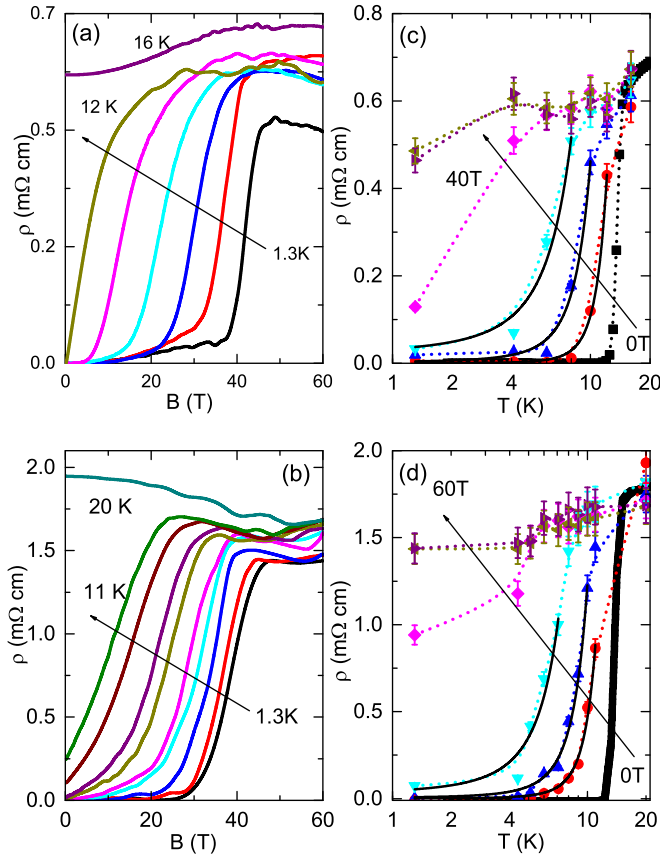


FIG. 2. Magnetic-field dependence of the in-plane resistivity at fixed temperatures for (a)  $\text{Fe}_{1.14}\text{Te}_{0.7}\text{Se}_{0.3}$  and (b)  $\text{Fe}_{1.02}\text{Te}_{0.61}\text{Se}_{0.39}$ . The arrows indicate the direction of increasing temperature. (a) For  $\text{Fe}_{1.14}\text{Te}_{0.7}\text{Se}_{0.3}$ , data were collected at 1.3, 4.0, 6.0, 8.0, 10.0, 12.1, and 16.0 K. (b) For  $\text{Fe}_{1.02}\text{Te}_{0.61}\text{Se}_{0.39}$ , data were collected at 1.3, 4.4, 5.1, 6.0, 7.1, 8.0, 9.0, 10.0, 11.0, and 20.0 K. Temperature dependence of the in-plane resistivity for (c)  $\text{Fe}_{1.14}\text{Te}_{0.7}\text{Se}_{0.3}$  and (d)  $\text{Fe}_{1.02}\text{Te}_{0.61}\text{Se}_{0.39}$ . The data were obtained from fixed-temperature pulsed magnetic-field sweeps. The arrows indicate the direction of increasing magnetic field: 0, 10, 20, 30, 40, 50, and 60 T. Note that 50- and 60-T data nearly overlap with each other in both (c) and (d).

similar to granular Al and  $\text{La}_{2-x}\text{Sr}_x\text{CuO}_4$  [6,13,51]. Within the framework of SIT theory in granular electronic systems, this is due to a competition between the gap opening in the density of states and the enhancement of conductance due to superconducting fluctuations [13]. In disordered InO, ultrathin TiN, or granular Al-Ge films the negative MR in high magnetic fields was explained by the destruction of fluctuation-related quasilocalized superconducting pairs [6,52,53]. In an array of superconducting grains in an insulating matrix, the magnetic field suppresses superconductivity in individual grains [13]. Above  $H_{c2}$ , virtual Cooper pairs can persist; they reduce the density of states (DOS) and cannot travel between grains, thus suppressing resistivity. This is the correction to the Drude resistivity due to DOS reduction. There are also Aslamazov-Larkin (transport channel via fluctuating Cooper pairs) and Maki-Thompson (coherent scattering of electrons forming Cooper pairs on impurities) corrections to Drude resistivity [54–57]. However, at low temperatures and in high magnetic fields  $H > H_{c2}$  the DOS reduction is dominant [13]. This leads

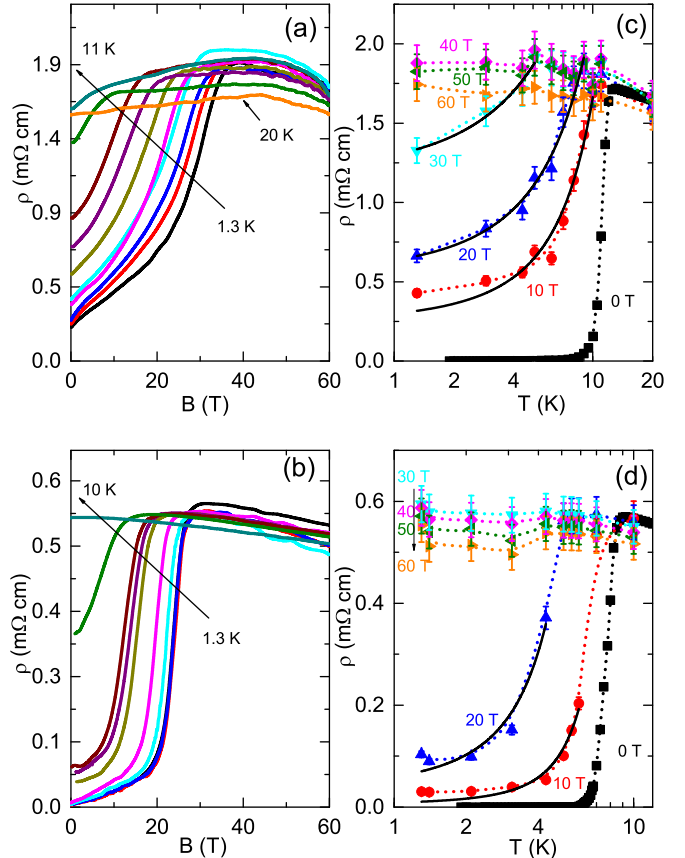


FIG. 3. Magnetic-field dependence of the in-plane resistivity vs magnetic field for (a)  $\text{Fe}_{1.05}\text{Te}_{0.89}\text{Se}_{0.11}$  and (b)  $\text{Fe}_{1.06}\text{Te}_{0.86}\text{S}_{0.14}$ . Temperature dependence of the in-plane resistivity for (c)  $\text{Fe}_{1.05}\text{Te}_{0.89}\text{Se}_{0.11}$  and (d)  $\text{Fe}_{1.06}\text{Te}_{0.86}\text{S}_{0.14}$ . The data were obtained from the results shown in panels (a,b). The arrows indicate the direction of increasing magnetic field: 0, 10, 20, 30, 40, 50, and 60 T.

to a negative MR especially at fields above  $H_{c2}$  of individual grains as seen experimentally in granular Al-Ge films [6].

In general, it should also be noted that the conductance  $g = 1/R$ , where  $R$  is the sample resistance of an inhomogeneous superconducting crystal such as granular aluminum films or  $\text{K}_x\text{Fe}_{2-y}\text{Se}_2$  can be approximated as  $g = g_{\text{SC}} + g_{\text{NSC}}$ , where  $g_{\text{SC}}$  and  $g_{\text{NSC}}$  are contributions from the superconducting and nonsuperconducting parts. In the superconducting state  $g_{\text{SC}}$  is infinite and  $g_{\text{NSC}}$  is short-circuited by the superconducting channel. In the normal state the nonsuperconducting grains may also contribute to the electronic transport when their conductivity is not very small when compared to superconducting grains.

In contrast to  $\text{K}_x\text{Fe}_{2-y}\text{Se}_2$ , which features phase separation where metallic grains ( $I4/mmm$  space group) are embedded in the insulating and magnetic matrix ( $I4/m$  space group) [17–21,32,33,58–61],  $\text{Fe}_{1+y}\text{Te}_{1-x}(\text{Se},\text{S})_x$  crystallize in a single space group without crystallographic phase separation, albeit with the presence of random excess interstitial Fe, inhomogeneous Fe-(Te,Se) bond lengths, i.e.,  $\text{Fe}(\text{Te},\text{Se})_4$  tetrahedra, due to deviations of the local structure from the average, and possible defects on the Te site [23,29–31,62]. On lowering

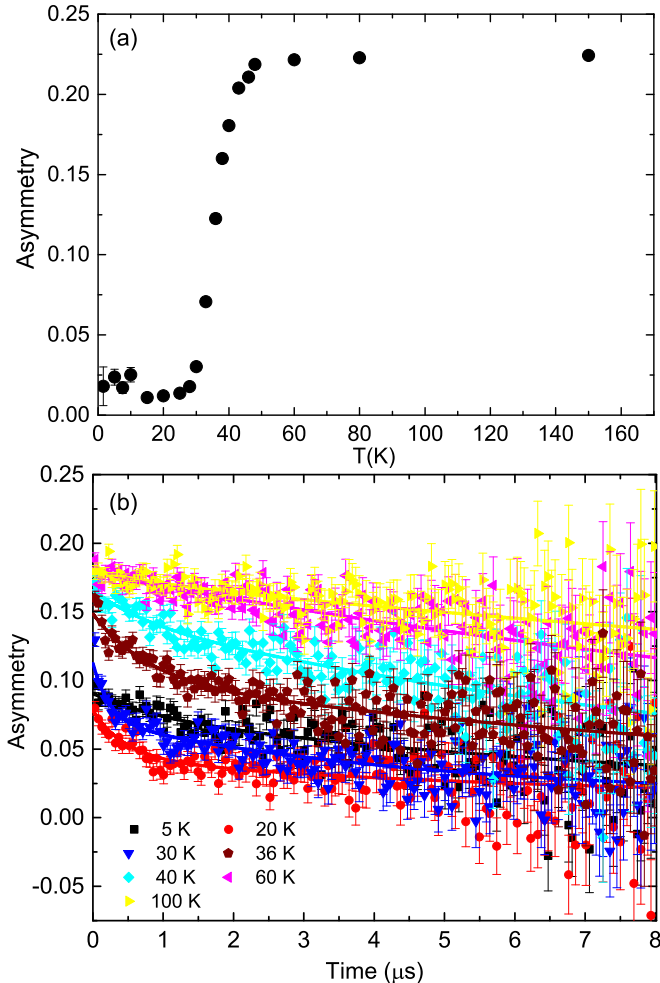


FIG. 4. (a) Amplitude of the precessing asymmetry signal in a weak transverse field (5 mT) for  $\text{Fe}_{1.12}\text{Te}_{0.83}\text{S}_{0.11}$ . The drop of the signal indicates bulk magnetism ( $\sim 100\%$  volume fraction) below 37 K. (b) Corresponding zero-field data showing the onset of magnetism below  $\sim 50$  K. Lines are fit to the time evolution of the polarization. See text for details.

the temperature, magnetism appears before superconductivity sets in for  $\text{Fe}_{1+y}\text{Te}_{1-x}(\text{Se},\text{S})_x$ ; however, magnetism coexists with superconductivity only in the superconducting state below  $T_c$  and  $H_{c2}$  [22]. In the normal state the two-phase electronic conduction is absent.

In addition to the electrical-transport measurements, we have performed  $\mu$ SR measurements on  $\text{Fe}_{1.12}\text{Te}_{0.83}\text{S}_{0.11}$  in order to probe the volume fraction of superconducting and magnetic phases.  $\text{Fe}_{1.12}\text{Te}_{0.83}\text{S}_{0.11}$  has a similar onset  $T_c$  as  $\text{Fe}_{1.06}\text{Te}_{0.88}\text{S}_{0.14}$  [8.6(1) versus 8.7(1) K], but lower zero-resistance  $T_c$  [3.5(1) versus 7.0(1) K] and only a small diamagnetic signal in the magnetic susceptibility indicating percolative superconductivity [23]. Figure 4(a) shows the temperature dependence of the amplitude of the muon spin precession asymmetry in a weak transverse field. This measurement allows us to determine the magnetic volume fraction of the sample. In a nonmagnetic environment the local field sensed by the muons is determined by the applied field and a weakly damped muon spin precession is observed. If a fraction of the sample becomes magnetic muons stopping

in that environment quickly depolarize since the local field is much larger than the applied field and this fraction does not contribute to the precessing amplitude. The observed asymmetry is therefore a measure of the nonmagnetic volume fraction of the sample. The drop in asymmetry [Fig. 4(a)] and the fast relaxation at early times in the zero-field polarization spectra [Fig. 4(b)] indicate a bulk magnetic transition at higher temperatures than the superconducting  $T_c$ . From Fig. 4(a) we determine the transition temperature  $T_m$  (defined by the 50% drop in amplitude) to be 37 K with an onset at 50 K. The volume fraction below the transition of the magnetic phase is nearly 100%. The fact that above 50 K the asymmetry reaches only 0.22 and not 0.26 as it should be in this experimental setup means that there are some magnetic impurities (probably clusters) producing a signal loss at all measured temperatures up to room temperature. A similar effect has been observed in many Fe-based superconductors [22]. Below  $\sim 15$  K, the  $\mu$ SR signal increases, reflecting a  $\sim 10\%$  nonmagnetic fraction below the temperature of  $T_c$  onset. This shows that superconductivity while only filamentary or localized competes with magnetism for the sample volume. We found by  $\mu$ SR studies a similar filamentary superconductivity but with higher  $T_m$  (50 K for 50% drop and 70-K onset temperature) and smaller bulk magnetic fraction in  $\text{Fe}_{1.12(3)}\text{Te}_{0.97(1)}\text{S}_{0.03(2)}$ . Overall the results indicate that, at least in this part of the phase diagram,  $\text{Fe}_{1+y}\text{Te}_{1-x}\text{S}_x$  features similar electronic granularity (phase separation) as the Se-substituted compounds below zero-field  $T_c$  [22].

In the superconducting region near the SIT when  $H < H_{c2}$ , the resistivity of a granular superconductors behaves as  $R = R_0 \exp(T/T_0)$  (“inverse Arrhenius law”) due to the destruction of quasilocalized Cooper pairs by superconducting fluctuations [12]. The resistivity between 10 T up to about  $H_{c2}$  (of 20–40 T) for all investigated crystals is in agreement [solid lines in Figs. 2(b), 2(d), 3(b), and 3(d)] with the bosonic SIT scenario, even in  $\text{Fe}_{1.14}\text{Te}_{0.7}\text{Se}_{0.3}$  and  $\text{Fe}_{1.02}\text{Te}_{0.61}\text{Se}_{0.39}$  where the resistivity saturates above 50 T below about 10 K [Figs. 2(b) and 2(d)].

Figure 5 shows the values of  $T_0$  from the  $R = R_0 \exp(T/T_0)$  fits for  $\text{Fe}_{1.14}\text{Te}_{0.7}\text{Se}_{0.3}$  [Fig. 2(c)],  $\text{Fe}_{1.02}\text{Te}_{0.61}\text{Se}_{0.39}$  [Fig. 2(d)],  $\text{Fe}_{1.05}\text{Te}_{0.89}\text{Se}_{0.11}$  [Fig. 3(c)], and  $\text{Fe}_{1.06}\text{Te}_{0.86}\text{S}_{0.14}$  [Fig. 3(d)]. Within the scope of SIT theory the energy scale  $T_0$  is related to the localization length  $\xi$  as  $T_0 \sim e^2/a\kappa\xi$  where  $\kappa$  is the effective dielectric constant and  $a$  is the average grain size [13]. As the magnetic field is increased from 10 to 30 T, the value of  $T_0$  increases for all investigated materials. This would correspond to a decrease in localization length, perhaps from coupled clusters of grains to a single grain [13]. The values of  $T_0$  and its increase in magnetic field are higher for  $\text{Fe}_{1.05}\text{Te}_{0.89}\text{Se}_{0.11}$  where the superconducting volume fraction is minute (about 1%) when compared to the other investigated crystals (10–20%).

Whereas magnetic domains are separate in space and coexist with superconductivity at the nano- to meso-scale in  $\text{K}_x\text{Fe}_{2-y}\text{Se}_2$  and some copper oxides [17,19,63], there is evidence for the two-order-parameter coexistence on the atomic scale in  $\text{Fe}_{1+y}\text{Te}_{1-x}(\text{Se},\text{S})_x$  below zero-field  $T_c$  [22]. Moreover, electronic transport in the normal state above zero-field  $T_c$  in  $\text{Fe}_{1+y}\text{Te}_{1-x}(\text{S})_x$  is dominated by an incoherent magnetic Kondo-type scattering that arises due to

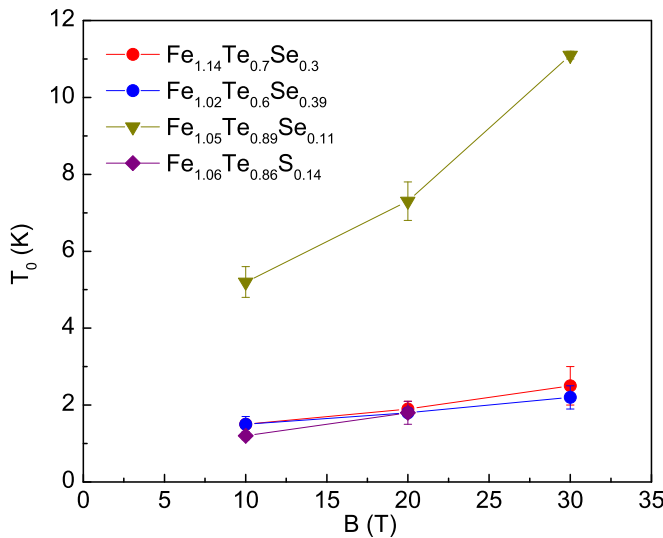


FIG. 5. Characteristic temperature  $T_0$  from the  $R = R_0 \exp(T/T_0)$  fits for  $\text{Fe}_{1.14}\text{Te}_{0.7}\text{Se}_{0.3}$ ,  $\text{Fe}_{1.02}\text{Te}_{0.6}\text{Se}_{0.39}$ ,  $\text{Fe}_{1.05}\text{Te}_{0.89}\text{Se}_{0.11}$ , and  $\text{Fe}_{1.06}\text{Te}_{0.86}\text{S}_{0.14}$  when resistivity is dominated by superconductivity in the context of SIT.

local-moment entanglement with itinerant electrons [39,40,64,65]. The local moments in  $\text{Fe}_{1+y}\text{Te}_{1-x}(\text{Se},\text{S})_x$  stem from the localized iron  $d$  orbitals in the  $\text{FeCh}_4$  tetrahedra as well as from the interstitial excess Fe ( $y$ ) [66]. However, it is plausible that pulsed magnetic fields of 60 T would suppress Kondo scattering given that the estimated value of Kondo temperature from scattering is about 24 K in  $\text{Fe}_{1+y}\text{Te}_{0.91}\text{S}_{0.09}$  and about 60 K in  $\text{FeTe}_{0.9}\text{Se}_{0.1}$  [39,67].

The chalcogen puckering in  $\text{FeCh}_4$  promotes itinerancy at the expense of localization [68,69]. A high-field nonmetallic normal state below  $T_c$  has been observed in  $\text{Fe}_{1.06}\text{Te}_{0.86}\text{S}_{0.14}$  (Fig. 3), which has less interstitial iron ( $y$ ) (outside of  $\text{FeCh}_4$ ) when compared to  $\text{Fe}_{1.14}\text{Te}_{0.7}\text{Se}_{0.3}$  [Fig. 2(c)] that is metallic

below  $T_c$ . In the absence of Kondo-type scattering, this could suggest less localized Fe- $d$  orbitals in  $\text{FeCh}_4$  in  $\text{Fe}_{1+y}(\text{Te},\text{Se})$  than  $\text{Fe}_{1+y}(\text{Te},\text{S})$ . This is consistent with the smaller anion height (i.e., smaller  $\text{FeCh}_4$  puckering) in  $\text{Fe}_{1+y}\text{Te}_{1-x}(\text{S})_x$  when compared to  $\text{Fe}_{1+y}\text{Te}_{1-x}(\text{Se})_x$  [70,71]. Therefore the SIT above  $H_{c2}$  and below  $T_c$  in  $\text{Fe}_{1.06}\text{Te}_{0.86}\text{S}_{0.14}$  is connected with the electronic phase separation.

#### IV. CONCLUSION

In summary, we have investigated the normal-state resistivity of  $\text{Fe}_{1.14}\text{Te}_{0.7}\text{Se}_{0.3}$ ,  $\text{Fe}_{1.02}\text{Te}_{0.61}\text{Se}_{0.39}$ ,  $\text{Fe}_{1.05}\text{Te}_{0.89}\text{Se}_{0.11}$ , and  $\text{Fe}_{1.06}\text{Te}_{0.86}\text{S}_{0.14}$  below  $T_c$  in pulsed magnetic fields. The  $\mu\text{SR}$  measurements confirm electronic phase separation in  $\text{Fe}_{1.06}\text{Te}_{0.86}\text{S}_{0.14}$ , similar to  $\text{Fe}_{1+y}\text{Te}_{1-x}\text{Se}_x$ . In contrast to  $\text{Fe}_{1.14}\text{Te}_{0.7}\text{Se}_{0.3}$  and  $\text{Fe}_{1.02}\text{Te}_{0.61}\text{Se}_{0.39}$ , the normal-state resistivity in  $\text{Fe}_{1.05}\text{Te}_{0.89}\text{Se}_{0.11}$  and  $\text{Fe}_{1.06}\text{Te}_{0.86}\text{S}_{0.14}$  shows clear SIT behavior below zero-field  $T_c$  in high magnetic fields above  $H_{c2}$  and is also nonmonotonic near  $H_{c2}$  as expected for a SIT in granular electronic systems [13].

#### ACKNOWLEDGMENTS

We thank I. Zaliznyak for useful discussions. Work at Brookhaven is supported by the Center for Emergent Superconductivity, an Energy Frontier Research Center funded by the U.S. Department of Energy, Office for Basic Energy Science (H.L. and C.P.). We acknowledge the support of Hochfeld-Magnetlabor Dresden at Helmholtz-Zentrum Dresden-Rossendorf, member of the European Magnetic Field Laboratory. C.P. acknowledges support by the Alexander von Humboldt Foundation. The  $\mu\text{SR}$  measurements have been performed at the Swiss Muon Source at the Paul Scherrer Institute. H.S. and E.M. acknowledge the financial support of the MaNEP program of the Swiss National Science Foundation.

- 
- [1] Z. P. Yin, K. Haule, and G. Kotliar, *Nat. Mater.* **10**, 932 (2011).
  - [2] P. Dai, J. Hu, and E. Dagotto, *Nat. Phys.* **8**, 709 (2012).
  - [3] L. de Medici, G. Giovannetti, and M. Capone, *Phys. Rev. Lett.* **112**, 177001 (2014).
  - [4] F. Hardy, A. E. Bohmer, D. Aoki, P. Burger, T. Wolf, P. Schweiss, R. Heid, P. Adelmann, Y. X. Yao, G. Kotliar, J. Schmalian, and C. Meingast, *Phys. Rev. Lett.* **111**, 027002 (2013).
  - [5] Y. Shapira and G. Deutscher, *Phys. Rev. B* **27**, 4463 (1983).
  - [6] A. Gerber, A. Milner, G. Deutscher, M. Karlovsky, and A. Gladlikh, *Phys. Rev. Lett.* **78**, 4277 (1997).
  - [7] K. M. Lang, V. Madhavan, J. E. Hoffman, H. Eisaki, S. Uchida, and J. C. Davis, *Nature (London)* **415**, 412 (2002).
  - [8] G. S. Boebinger, Y. Ando, A. Passner, T. Kimura, M. Okuya, J. Shimoyama, K. Kishio, K. Tamasaku, N. Ichikawa, and S. Uchida, *Phys. Rev. Lett.* **77**, 5417 (1996).
  - [9] S. Ono, Y. Ando, T. Murayama, F. F. Balakirev, J. B. Betts, and G. S. Boebinger, *Phys. Rev. Lett.* **85**, 638 (2000).
  - [10] P. Fournier, P. Mohanty, E. Maiser, S. Darzens, T. Venkatesan, C. J. Lobb, G. Czjzek, R. A. Webb, and R. L. Greene, *Phys. Rev. Lett.* **81**, 4720 (1998).
  - [11] M. Wallin, E. S. Sorensen, S. M. Girvin, and A. P. Young, *Phys. Rev. B* **49**, 12115 (1994).
  - [12] V. F. Gantmakher and V. T. Dolgopolov, *Phys. Usp.* **53**, 1 (2010).
  - [13] I. S. Beloborodov, A. V. Lopatin, V. M. Vinokur, and K. B. Efetov, *Rev. Mod. Phys.* **79**, 469 (2007).
  - [14] J. C. S. Davis and D. H. Lee, *Proc. Natl. Acad. Sci. USA* **110**, 17623 (2013).
  - [15] Q. Si and E. Abrahams, *Phys. Rev. Lett.* **101**, 076401 (2008).
  - [16] S. C. Riggs, J. B. Kemper, Y. Jo, Z. Stegen, L. Balicas, G. S. Boebinger, F. F. Balakirev, A. Migliori, H. Chen, R. H. Liu, and X. H. Chen, *Phys. Rev. B* **79**, 212510 (2009).
  - [17] D. H. Ryan, W. N. Rowan-Weetaluktuk, J. M. Cadogan, R. Hu, W. E. Straszheim, S. L. Bud'ko, and P. C. Canfield, *Phys. Rev. B* **83**, 104526 (2011).
  - [18] W. Bao, Q. Z. Huang, G. F. Chen, M. A. Green, D. M. Wang, J. B. He, and Y. M. Qiu, *Chin. Phys. Lett.* **28**, 086104 (2011).
  - [19] W. Li, H. Ding, P. Deng, K. Chang, C. Song, Ke He, L. Wang, X. Ma, J. P. Hu, X. Chen, and Q. K. Xue, *Nat. Phys.* **8**, 126 (2012).
  - [20] F. Chen, M. Xu, Q. Q. Ge, Y. Zhang, Z. R. Ye, L. X. Yang, J. Jiang, B. P. Xie, R. C. Che, M. Zhang, A. F. Wang,

- X. H. Chen, D. W. Shen, J. P. Hu, and D. L. Feng, *Phys. Rev. X* **1**, 021020 (2011).
- [21] R. H. Yuan, T. Dong, Y. J. Song, P. Zheng, G. F. Chen, J. P. Hu, J. Q. Li, and N. L. Wang, *Sci. Rep.* **2**, 221 (2012).
- [22] R. Khasanov, M. Bendele, A. Amato, P. Babkevich, A. T. Boothroyd, A. Cervellino, K. Conder, S. N. Gvasaliya, H. Keller, H.-H. Klauss, H. Luetkens, V. Pomjakushin, E. Pomjakushina, and B. Roessli, *Phys. Rev. B* **80**, 140511 (2009).
- [23] R. Hu, E. S. Bozin, J. B. Warren, and C. Petrovic, *Phys. Rev. B* **80**, 214514 (2009).
- [24] X. He, G. Li, J. Zhang, A. B. Karki, R. Jin, B. C. Sales, A. S. Sefat, M. A. McGuire, D. Mandrus, and E. W. Plummer, *Phys. Rev. B* **83**, 220502 (2011).
- [25] H. Hu, J.-M. Zuo, J. Wen, Z. Xu, Z. Lin, Q. Li, G. Gu, W. K. Park, and L. H. Greene, *New J. Phys.* **13**, 053031 (2011).
- [26] S. Li, C. de la Cruz, Q. Huang, Y. Chen, J. W. Lynn, J. Hu, Yi-Lin Huang, Fong-Chi Hsu, Kuo-Wei Yeh, Maw-Kuen Wu, and P. Dai, *Phys. Rev. B* **79**, 054503 (2009).
- [27] K. Horigane, H. Hiraka, and K. Ohoyama, *J. Phys. Soc. Jpn.* **78**, 074718 (2009).
- [28] K.-W. Yeh, T. W. Huang, Y. L. Huang, T. K. Chen, F. C. Hsu, P. M. Wu, Y. C. Lee, Y. Y. Chu, C. L. Chen, J. Y. Luo, D. C. Yan, and M. K. Wu, *Europhys. Lett.* **84**, 37002 (2008).
- [29] A. Iadecola, B. Joseph, A. Puri, L. Simonelli, Y. Mizuguchi, D. Testemale, O. Proux, J.-L. Hazemann, Y. Takano, and N. L. Saini, *J. Phys. Condens. Matter* **23**, 425701 (2011).
- [30] D. Louca, K. Horigane, A. Llobet, R. Arita, S. Ji, N. Katayama, S. Konbu, K. Nakamura, T.-Y. Koo, P. Tong, and K. Yamada, *Phys. Rev. B* **81**, 134524 (2010).
- [31] B. Joseph, A. Iadecola, A. Puri, L. Simonelli, Y. Mizuguchi, Y. Takano, and N. L. Saini, *Phys. Rev. B* **82**, 020502 (2010).
- [32] K. F. Wang, H. Ryu, E. Kampert, M. Uhlarz, J. Warren, J. Wosnitza, and C. Petrovic, *Phys. Rev. X* **4**, 031018 (2014).
- [33] H. Ryu, F. Wolff-Fabris, J. B. Warren, M. Uhlarz, J. Wosnitza, and C. Petrovic, *Phys. Rev. B* **90**, 020502(R) (2014).
- [34] P. B. Allen, W. E. Pickett, and H. Krakauer, *Phys. Rev. B* **37**, 7482 (1988).
- [35] F. C. Hsu, J. Y. Luo, K. W. Yeh, T. K. Chen, T. W. Huang, P. M. Wu, Y. C. Lee, Y. L. Huang, Y. Y. Chu, D. C. Yan, and M. K. Wu, *Proc. Natl. Acad. Sci. USA* **105**, 14262 (2008).
- [36] S. Medvedev, T. M. McQueen, I. A. Troyan, T. Palasyuk, M. I. Eremets, R. J. Cava, S. Naghavi, F. Casper, V. Ksenofontov, G. Wortmann, and C. Felser, *Nat. Mater.* **8**, 630 (2009).
- [37] J. Guo, S. Jin, G. Wang, S. Wang, K. Zhu, T. Zhou, M. He, and X. Chen, *Phys. Rev. B* **82**, 180520(R) (2010).
- [38] J. F. Ge, Z. L. Liu, C. H. Liu, C. L. Gao, D. Qian, Q. K. Xue, Y. Liu, and J. F. Jia, *Nat. Mater.* **14**, 258 (2015).
- [39] H. Lei, R. Hu, E. S. Choi, J. B. Warren, and C. Petrovic, *Phys. Rev. B* **81**, 184522 (2010).
- [40] I. A. Zaliznyak, Z. Xu, J. M. Tranquada, G. Gu, A. M. Tsvelik, and M. B. Stone, *Phys. Rev. Lett.* **107**, 216403 (2011).
- [41] H. Lei, R. Hu, E. S. Choi, J. B. Warren, and C. Petrovic, *Phys. Rev. B* **81**, 094518 (2010).
- [42] A. Suter and B. M. Wojek, *Physics Procedia* **30**, 69 (2012).
- [43] N. Stojilovic, A. Koncz, L. W. Kohlman, R. Hu, C. Petrovic, and S. V. Dordevic, *Phys. Rev. B* **81**, 174518 (2010).
- [44] H. Lei and C. Petrovic, *Phys. Rev. B* **83**, 184504 (2011).
- [45] Y. Liu, R. K. Kremer, and C. T. Lin, *Supercond. Sci. Technol.* **24**, 035012 (2011).
- [46] O. Gunnarson, M. Calandra, and J. E. Han, *Rev. Mod. Phys.* **75**, 1085 (2003).
- [47] N. E. Hussey, K. Takenaka, and H. Takagi, *Philos. Mag.* **84**, 2847 (2004).
- [48] P. L. Bach, S. R. Saha, K. Kirshenbaum, J. Paglione, and R. L. Greene, *Phys. Rev. B* **83**, 212506 (2011).
- [49] J. L. Her, Y. Kohama, Y. H. Matsuda, K. Kindo, W.-H. Yang, D. A. Chareev, E. S. Mitrofanova, O. S. Volkova, A. N. Vasiliev, and J.-Y. Lin, *Supercond. Sci. Technol.* **28**, 045013 (2015).
- [50] S. I. Vedeneev, B. A. Piot, D. K. Maude, and A. V. Sadakov, *Phys. Rev. B* **87**, 134512 (2013).
- [51] Y. Ando, G. S. Boebinger, A. Passner, T. Kimura, and K. Kishio, *Phys. Rev. Lett.* **75**, 4662 (1995).
- [52] M. A. Paalanen, A. F. Hebard, and R. R. Ruel, *Phys. Rev. Lett.* **69**, 1604 (1992).
- [53] T. I. Baturina, C. Strunk, M. R. Baklanov, and A. Satta, *Phys. Rev. Lett.* **98**, 127003 (2007).
- [54] L. G. Aslamazov and A. I. Larkin, *Sov. Phys. Solid State* **10**, 875 (1968).
- [55] K. Maki, *Prog. Theor. Phys.* **39**, 897 (1968).
- [56] K. Maki, *Prog. Theor. Phys.* **40**, 193 (1968).
- [57] R. S. Thompson, *Phys. Rev. B* **1**, 327 (1970).
- [58] D. Louca, K. Park, B. Li, J. Neufeind, and J. Yan, *Sci. Rep.* **3**, 2047 (2013).
- [59] Z. Wang, Y. J. Song, H. L. Shi, Z. W. Wang, Z. Chen, H. F. Tian, G. F. Chen, J. G. Guo, H. X. Yang, and J. Q. Li, *Phys. Rev. B* **83**, 140505 (2011).
- [60] X. Ding, D. Fang, Z. Wang, H. Yang, J. Liu, Q. Deng, G. Ma, and C. Meng, *Nat. Commun.* **4**, 1897 (2013).
- [61] Z. Wang, Y. Cai, Z. W. Wang, C. Ma, Z. Chen, H. X. Yang, H. F. Tian, and J. Q. Li, *Phys. Rev. B* **91**, 064513 (2015).
- [62] S. Rössler, D. Cherian, S. Harikrishnan, H. L. Bhat, S. Elizabeth, J. A. Mydosh, L. H. Tjeng, F. Steglich, and S. Wirth, *Phys. Rev. B* **82**, 144523 (2010).
- [63] A. T. Savici, Y. Fudamoto, I. M. Gat, T. Ito, M. I. Larkin, Y. J. Uemura, G. M. Luke, K. M. Kojima, Y. S. Lee, M. A. Kastner, R. J. Birgeneau, and K. Yamada, *Phys. Rev. B* **66**, 014524 (2002).
- [64] I. A. Zaliznyak, A. T. Savici, M. Lumsden, A. Tsvelik, R. Hu, and C. Petrovic, *Proc. Natl. Acad. Sci. USA* **112**, 10316 (2015).
- [65] S. Ducatman, R. M. Fernandes, and N. B. Perkins, *Phys. Rev. B* **90**, 165123 (2014).
- [66] A. Subedi, L. Zhang, D. J. Singh, and M. H. Du, *Phys. Rev. B* **78**, 134514 (2008).
- [67] M. B. Salamon, N. Cornell, M. Jaime, F. F. Balakirev, A. Zakhidov, J. Huang, and H. Wang, *Sci. Rep.* **6**, 21469 (2015).
- [68] V. Cvetkovic and Z. Tesanovic, *Europhys. Lett.* **85**, 37002 (2009).
- [69] L. Zhang, D. J. Singh, and M. H. Du, *Phys. Rev. B* **79**, 012506 (2009).
- [70] H. Okabe, N. Takeshita, K. Horigane, T. Muranaka, and J. Akimitsu, *Phys. Rev. B* **81**, 205119 (2010).
- [71] Y. Mizuguchi, Y. Hara, K. Deguchi, S. Tsuda, T. Yamaguchi, K. Takeda, H. Kotegawa, H. Tou, and Y. Takano, *Supercond. Sci. Technol.* **23**, 054013 (2010).